

Clouds and the Earth's Radiant Energy System (CERES)

Validation Plan

CERES Inversion to Instantaneous TOA Fluxes

(Subsystem 4.5)

N. G. Loeb¹
R. N. Green²
L. H. Chambers²
B. A. Wielicki²
Y. Hu¹
J. A. Coakley III³
L. L. Stowe⁴
P. O'R. Hinton⁵

¹Hampton University-NASA Langley Research Center, Hampton, Virginia 23681-0001

²Atmospheric Sciences Division, NASA Langley Research Center, Hampton, Virginia 23681-0001

³Oregon State University, Corvallis, Oregon 97331-2209

⁴NOAA/NESDIS/E/RALL, 5200 Auth Road, Camp Springs, Maryland 20233

⁵Science Applications International Corporation (SAIC), Hampton, Virginia 23666

CERES INVERSION TO INSTANTANEOUS TOA FLUXES

4.5.1 INTRODUCTION

There are several steps in converting measured radiances into flux at the TOA. The first step is to apply the Spectral Correction Algorithm (ATBD 2.2.1) to convert filtered radiances from each channel to unfiltered radiances of shortwave and longwave. The validity of both the algorithm and the radiance measurements are discussed in Section 2.0. Next, we must know the scene type of the area we are examining so that the proper Angular Distribution Model (ADM) can be used. The cloud parameters that define the scene type are validated in Subsections 4.1 - 4.3 and averaged over the CERES footprint in Subsection 4.4. And finally the unfiltered radiances are inverted to the top of the atmosphere (TOA) by

$$\hat{F}_j = \frac{\pi I_j}{\hat{R}_i(\Omega)} \quad (4.5-1)$$

where I_j (j =SW, LW, WN) are the CERES unfiltered radiances, \hat{F}_j are the corresponding flux estimates at the TOA, and $\hat{R}_i(\Omega)$ are the angular distribution models (ADM) that relate radiance to flux for the i th scene type. This section will concentrate on the validation of the TOA flux estimates derived from ADMs.

The CERES radiances will be inverted with two different sets of ADMs and scene identifications. In Section 2.0 we validate the ERBE-like inversion to the TOA fluxes using the Maximum Likelihood Estimation (MLE) technique (Wielicki and Green 1989) and the ERBE ADMs with 12 scene types (Suttles et al. 1988, 1989). In this section we are concerned with the inversion to TOA fluxes using cloud parameters (Subsection 4.1-4.3) to define the scene type and a new set of CERES ADM scene types. These new ADMs will be constructed from CERES radiance data.

4.5.1.1 Measurement and science objectives

The CERES scanning radiometers measure the earth radiance in three spectral bands and are discussed in Section 1.1.1. We will refer to these measurements as the shortwave (SW), total (TOT), and window (WN) measurements.

The CERES ADMs will be constructed from CERES radiances measurements using the Sorting-into-Angular Bins (SAB) approach (see Suttles et al., 1992).

4.5.1.2 Missions

The CERES scanners will be launched aboard the TRMM spacecraft and the EOS AM and PM platforms (see Section 1.1.2)

4.5.1.3 Science data products

The science data product for this section is the instantaneous TOA flux as recorded on the Single Satellite Footprint Product (SSF) (ATBD Section 4.0 App. B-3) which also contains measurement time, viewing geometry, CERES radiances, imager radiances, scene type, TOA fluxes, surface fluxes, and cloud statistics.

4.5.2 VALIDATION CRITERION

4.5.2.1 Overall approach

Validation will play a central role during the development of new CERES ADMs. As new CERES scene types are defined, the validation techniques outlined below will be used to assess the accuracy of CERES TOA fluxes for a subset of scene types. The validation results will act as a guide in identifying conditions where further refinement of CERES ADM scene types are required. For example, while it is clear that increasing the number of ADM scene types according to optical properties will reduce instantaneous and regional mean flux errors, there is no way to determine *a priori* the optimal set of properties and the manner in which they should be stratified. Model simulations provide a useful guide in determining which properties are likely to be important, but ultimately, the final set of ADM scene types must be defined and validated through observations. By incorporating the following validation techniques as a crucial step in the development of new CERES ADMs (i.e. in an iterative manner), it will be possible to derive an optimal set of CERES TOA ADMs that meet the CERES TOA flux accuracy requirements.

We will use several different tests to validate the ADM-derived TOA fluxes. The Direct Integration method determines the monthly regional flux without scene identification or ADMs. It is compared to the normal ADM inversion and differences are considered to be due to ADM errors. The Viewing Zenith Angle Dependence Test collects a large ensemble of radiance data stratified by viewing geometry to examine whether mean fluxes are self-consistent in all angles. Similarly, the Along-Track Test collects instantaneous radiance data along the ground track from multiple angles over the same area. Since the same area is viewed from different angles, the derived fluxes should be identical. Any differences in flux between the angles must be due to ADM uncertainties. Finally, throughout the ADM development-validation process, we will conduct theoretical modeling studies to improve our understanding of the underlying physics of how scene optical properties influence scene anisotropy and TOA flux estimation.

4.5.2.1.1 Direct Integration Method

The Direct Integration Method involves a consistency check between ADM-derived monthly mean regional fluxes and mean fluxes inferred by direct integration of the mean radiance field. All radiances over a month are sorted into angular bins for a given region, averaged, and then integrated over the angular bins to determine a monthly regional flux. The CERES scanner in the

Rotating Azimuth Plane mode (RAP) will provide the angular sampling necessary to perform this comparison. The direct integration results are compared with the average of all instantaneous flux estimates of the same region using the ADM inversion. Both methods use the same data, but one uses ADMs while the other does not. Under ideal conditions, both methods should provide the same results. Fluxes inferred by direct integration are taken as truth since they are independent of ADMs. Any differences are considered ADM errors.

It should be pointed out that fluxes inferred by direct integration are not true monthly average fluxes because no diurnal effects have been considered. These results are instead the average of all monthly sampling. CERES incorporates diurnal effects in its time averaging and needs instantaneous fluxes, so that direct integration results are of no help. Rather, the main use of the direct integration method is for validation of ADM-derived mean regional fluxes.

To illustrate the effectiveness of the direct integration method, Figs. 1 and 2 show monthly regional mean albedos (for November, 1996) determined for all $10^\circ \times 10^\circ$ latitude/longitude regions over ocean between 60°S and 60°N for different solar zenith angle ranges. These results were obtained by using ADMs based on two months of POLDER (Polarization and Directionality of Earth's Reflectances) 670 nm radiances. Scene types for these ADMs are defined for discrete intervals of cloud fraction and cloud optical depth (see Table 1). Recognizing that 1D-derived cloud optical depth often show significant biases that depend on viewing geometry (Loeb and Davies, 1996; Loeb and Coakley, 1997), two sets of ADMs are considered: i) fixed- τ ADMs use fixed cloud optical depth classes in all angles; the percentile- τ ADMs use percentiles of cloud optical depth in each angular bin (Loeb et al., 1999a). Also provided are albedos inferred from 1D theory averaged over all POLDER instantaneous views (up to 14) of each target (POLDER 1D Mult-View). To reduce sampling noise, only regions having samples in each angular bin from a minimum of 7 days out of the month were considered. As noted above, albedos inferred by direct integration is taken as the true albedo.

As shown, overall biases for the monthly regional albedos (Fig. 2a) are $< 0.5\%$ (relative) for the percentile- τ approach. 2σ differences in monthly regional albedos based on ADMs are $< 4\%$ (relative), a factor of 2 smaller than those based on the POLDER 1D multiple-view approach for solar zenith angles $< 50^\circ$.

Suttles et al. (1992) compared global ERBE ADM albedos over $500 \text{ km} \times 500 \text{ km}$ regions with albedos inferred by direct integration (which they refer to as the "SAB" method). ERBE ADM albedos showed a bias of 1.5% (relative) and a regional RMS difference of 6% (relative). The corresponding values from the present study (obtained by averaging results in Fig. 2 over all solar zenith angles) for the percentile- τ approach are 0.15% and 1.5% , a reduction by a factor 10 in bias error and a factor of 4 in RMS error. While part of the reduction in error may be due to the different sampling strategy used in determining the regional mean albedos (i.e. equal angle weighting), a more important consideration is likely the number of scene types considered: ERBE considered only four classes of cloud cover (clear, partly cloudy, mostly cloudy and overcast) compared to 19 in the present study. The larger number of scene types improves albedo estimates by increasing ADM sensitivity to scene parameters that have the greatest influence on anisotropy. Interestingly, the reduction in error based on the current set of 19 ADMs (compared to ERBE) is consistent with the expected reduction in error for CERES albedos based on a new set of CERES ADMs defined for a larger set of scene types (Wielicki et al., 1995).

Once the new CERES ADMs have been developed, the Direct Integration Method will be adopted to assess errors in mean regional fluxes over the entire globe.

Cloud Fraction Interval (%)	Cloud Opt Depth Interval	Cloud Opt Depth Percentile Interval	Total
0 - 1	All	0 – 100	1
1 - 25	0 – 1.5 > 1.5	0 – 50 50 - 100	2
25 - 50	0 – 1.5 > 1.5	0 – 50 50 – 100	2
50 - 75	0 – 1 1 – 2.5 > 2.5	0.0 – 33.3 33.3 – 66.6 66.6 – 100	3
75 - 99	0 – 1 1 – 2 2 – 3 3 – 5 > 5	0.0 – 20 20 – 40 40 – 60 60 – 80 80 – 100	5
99 - 100	0 - 2.5 2.5 - 6 6 - 10 10 - 18 18 - 40 > 40	0 – 5 5 – 25 25 – 50 50 – 75 75 – 95 95 – 100	6

Table 4.5-1 Cloud fraction and cloud optical depth intervals defining ADM scene-types.

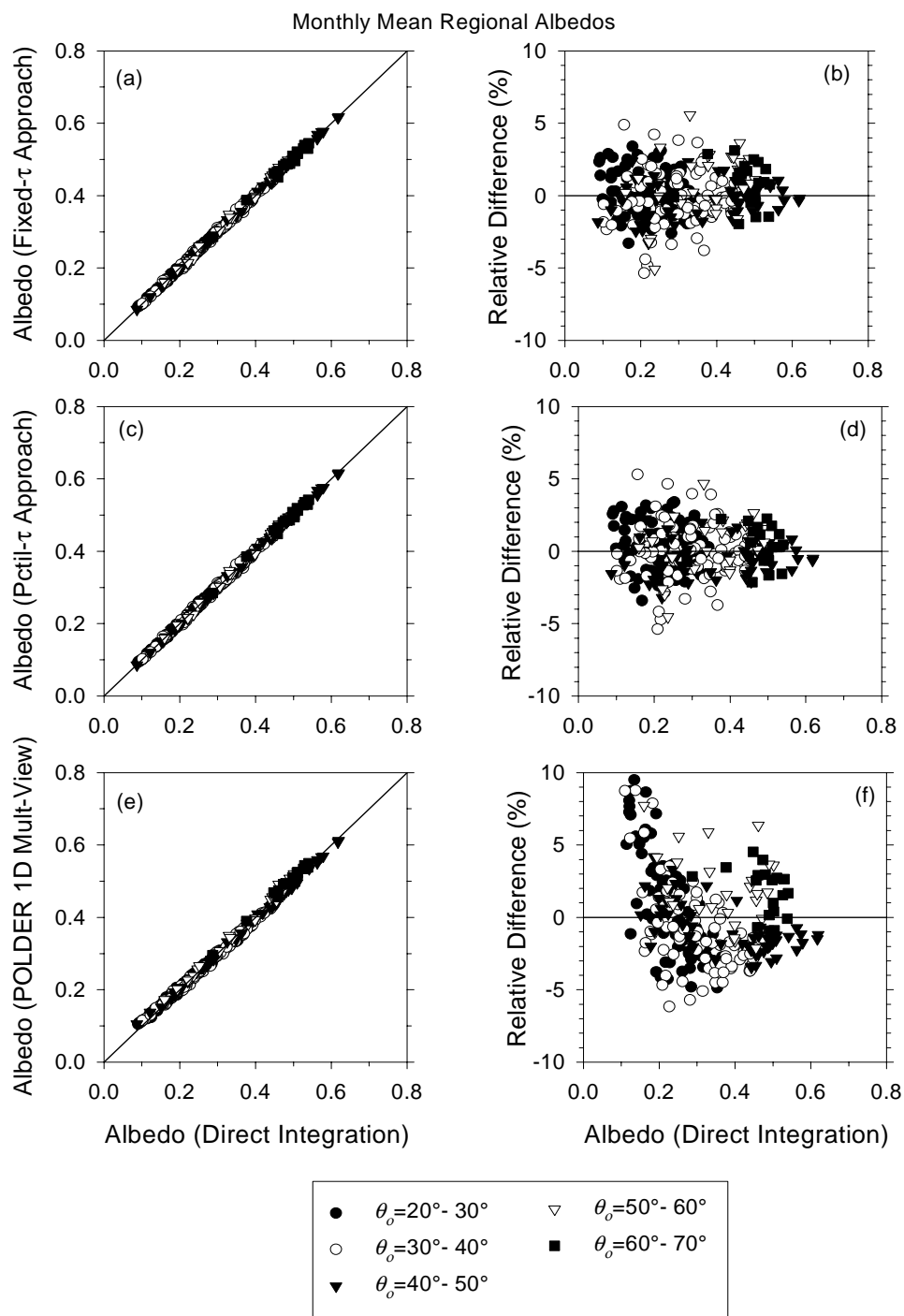


Figure 1 Monthly regional mean albedos and relative differences (compared to direct integration albedo) for fixed- τ (Figs. 1a-b), percentile- τ (Figs. 1c-d) and the POLDER 1D multiple view (Figs. 1e-f) approaches for $10^\circ \times 10^\circ$ regions as a function of solar zenith angle.

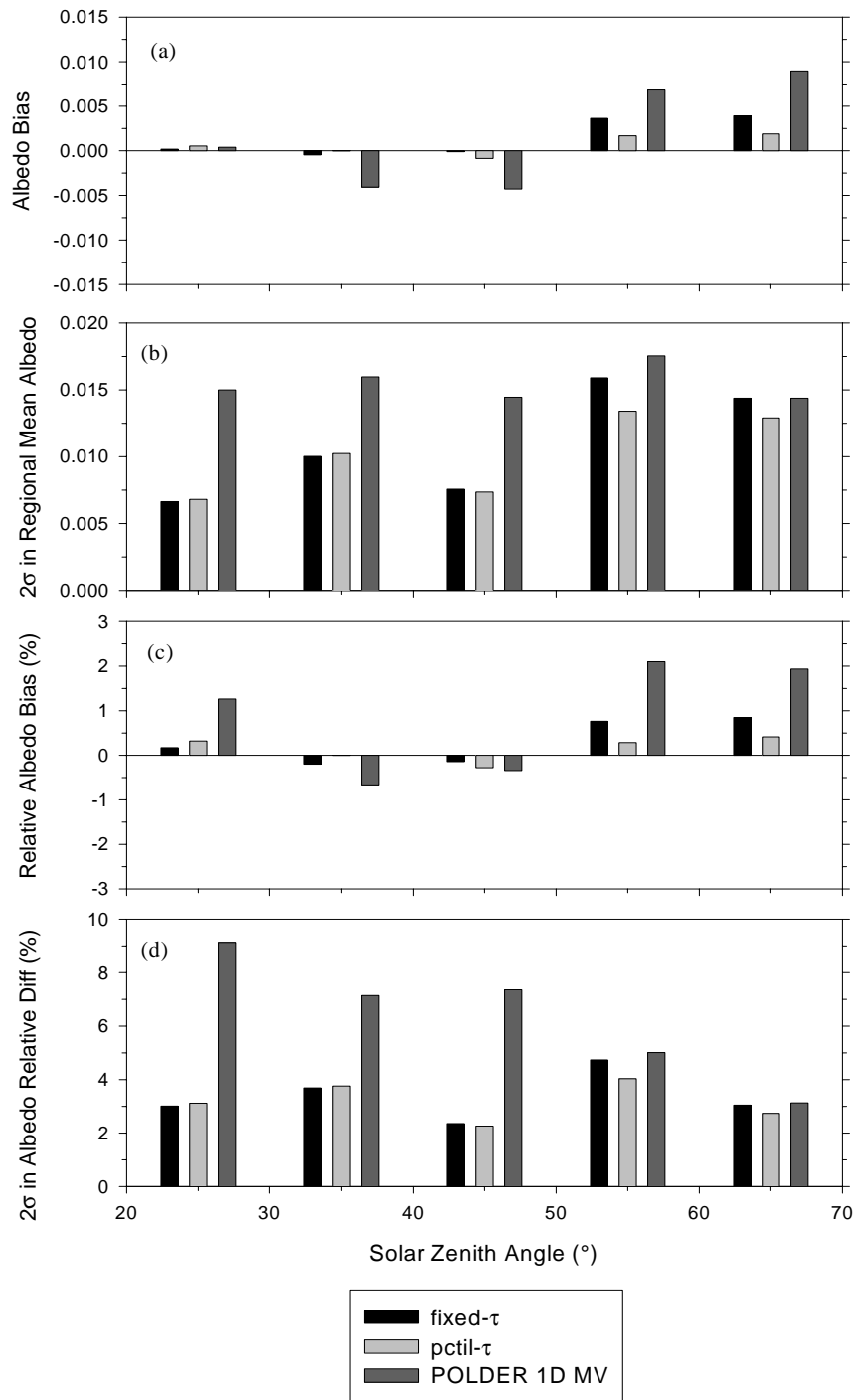


Figure 2 Bias, relative bias and 2σ difference (2σ =standard deviation in estimated-direct integration albedos) for monthly regional mean albedos plotted in Fig. 1.

4.5.2.1.2 Viewing Zenith Angle Dependence Test

Another method of validating ADM-derived albedos is to test whether the mean albedos show any dependence on viewing zenith angle. If a large ensemble (e.g. months) of albedos for a given population are stratified by viewing zenith angle, the means should be independent of the viewing geometry. Figs. 3a-f show mean albedos and mean cloud optical depth retrievals for solar zenith angles between 20°-30° (Figs. 3a-b), 40°-50° (Figs. 3c-d) and 60°-70° (Figs. 3e-f) for overcast POLDER measurements (cloud fraction >0.99). The mean albedos were determined for both the fixed- τ and percentile- τ approaches as a function of viewing zenith angle. These are compared with ADM albedos averaged over all angles, and albedos obtained by direct integration. To reduce sampling differences between the direct integration and ADM albedos, the ADM albedos were averaged in a manner that mimics that used in determining albedo by direct integration: mean albedos for each viewing zenith-relative azimuth angle bin combination are determined first. Next, mean albedos as a function of viewing zenith angle and mean albedo over all angles are obtained by averaging the bin-averaged albedos (i.e. so that each angular bin contributes equal weight to the overall mean).

As shown in Figs. 3a, 3c and 3e, albedos inferred based on the fixed- τ approach show a large dependence on viewing zenith angle. The viewing zenith angle dependence closely follows that obtained for the mean cloud optical depth retrievals (Figs. 3b, 3d and 3f), and becomes more pronounced with increasing solar zenith angle—fixed- τ albedos decrease by as much as $\approx 15\%$ between near-nadir and oblique viewing zenith angles for $\theta_o=60^\circ-70^\circ$. These results clearly demonstrate how scene identification errors in cloud property retrievals can introduce errors in ADM-derived albedos. In contrast, albedos based on the percentile- τ approach show very little viewing zenith angle dependence, and are in good agreement with the direct integration albedo. Interestingly, when albedos are averaged over all angles (i.e. all relative azimuth and viewing zenith angle bins), much of the albedo error with viewing zenith angle that occurs in the fixed- τ approach cancels, and the resulting mean albedo is much closer to that obtained by direct integration.

Figures 4a-f show similar results to those in Figs. 3a-f, but for all scenes. Also, mean cloud fraction retrievals are provided in Figs. 4b, 4d and 4f instead of mean cloud optical depth. As shown, the viewing zenith angle dependence in mean cloud fraction retrievals is much less pronounced than that in mean cloud optical depth (Figs. 3b, 3d and 3f). Because fixed absolute intervals of cloud fraction were used to define the ADM scene types, albedos based on the percentile- τ approach show a slight variation ($< 6\%$, relative) with viewing zenith angle (Figs. 4a, 4c and 4e) which closely follows the viewing zenith angle dependence in mean cloud fraction. In contrast, mean albedos based on the fixed- τ approach vary by as much as $\approx 15-20\%$ (relative) with viewing zenith angle, owing to the additional viewing zenith angle bias in cloud optical depth.

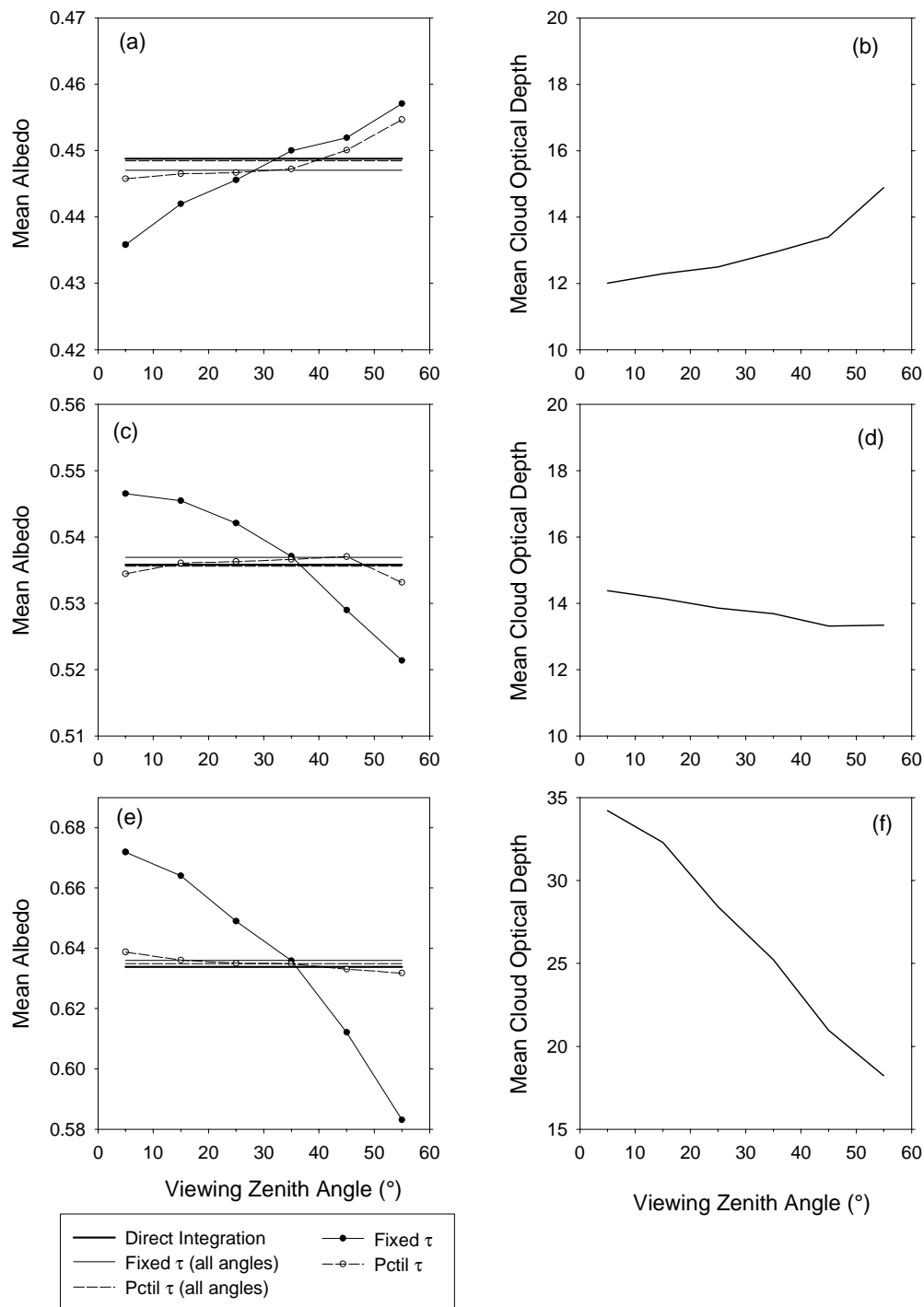


Figure 3 Mean albedos (left) and mean retrieved cloud optical depths (right) against viewing zenith angle for θ_o between 20°-30° (Figs. 3a-b), 40°-50° (Figs. 3c-d) and 60°-70° (Figs. 3e-f).

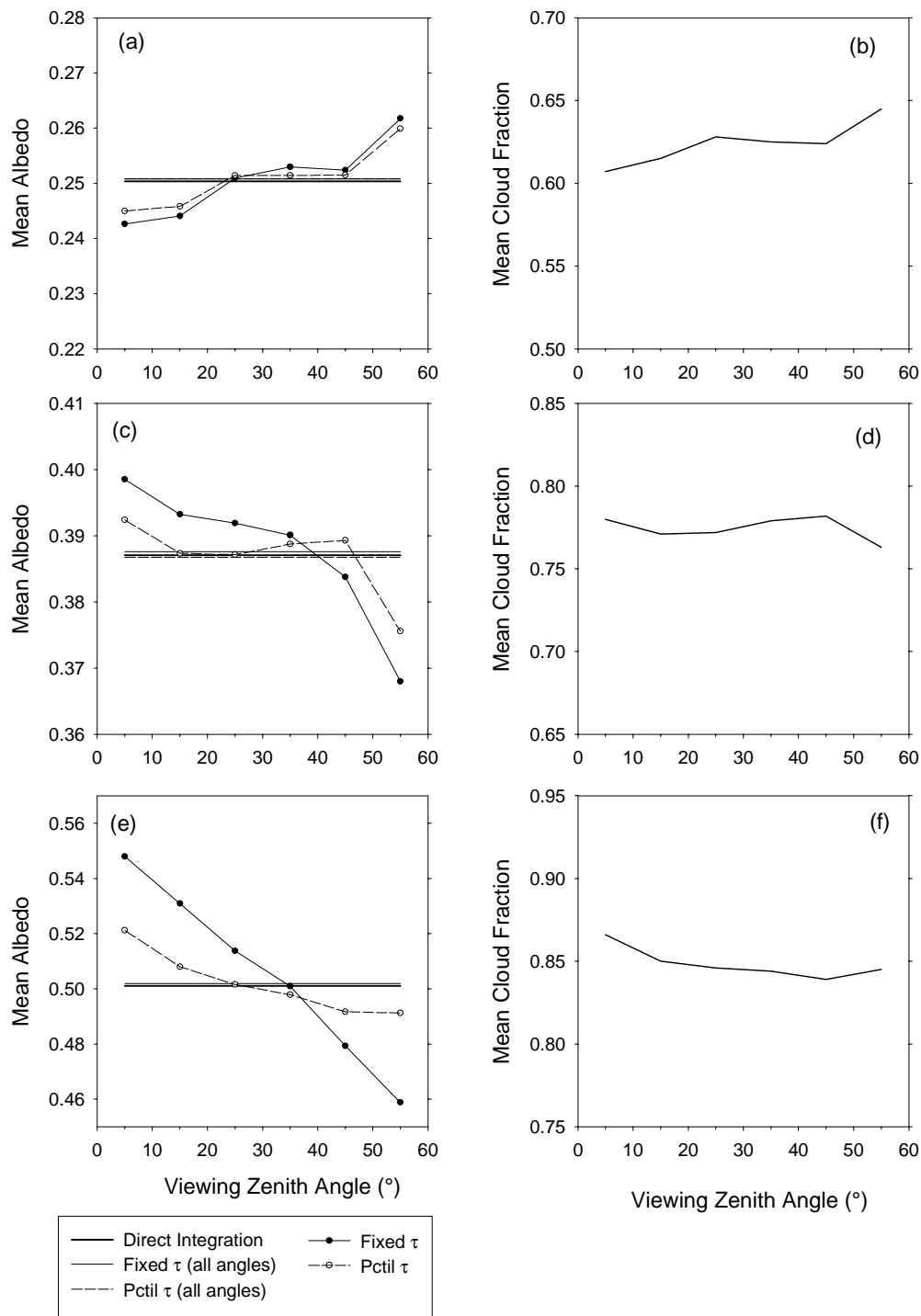


Figure 4 Mean albedos (left) and mean cloud fractions (right) against viewing zenith angle for θ_0 between 20°-30° (Figs. 4a-b), 40°-50° (Figs. 4c-d) and 60°-70° (Figs. 4e-f).

4.5.2.1.3 Along-track Test

The purpose of the ADMs are to remove the angular dependence from the radiance to flux conversion. A test of the ADM to accomplish this is to determine the TOA flux as a function of the viewing zenith. A valid set of ADMs should produce near constant flux independent to the viewing angles. The ERBE mission has produced several special along-track data sets for this purpose (Smith et al. 1989a, 1989b, 1990). From August 3 to 9, 1985 the ERBS scanning radiometer was rotated in azimuth to scan along track in the plane of the orbit. In this mode the scanner views a site along the ground track from a full range of viewing zenith angles and we can determine the flux for different angles. Green et al. 1990 has shown that this data and the ERBE12 ADMs resulted in a 10-15% albedo rise from nadir to the limb which agrees with the Suttles SAB results using Nimbus-7 data. The great advantage of the along-track data is that we are assured that each viewing zenith data set views the same along-track area so that it should get the same flux without having to rely on long-term data averaging. Any drop in the longwave flux from nadir to limb can be associated with an ADM limb-darkening error. For shortwave we only sample a slice through the viewing zenith-azimuth hemisphere. However, knowing the variance of the ADMs, we can test that this realization falls within the expected range.

4.5.2.1.4 CERES-MISR-POLDER-GERB Intercomparisons

Several other instruments will provide complementary Earth radiation budget observations that will be useful for validation studies. MISR (Multiangle Imaging Spectroradiometer) will fly on the EOS-AM platform together with CERES in July, 1999. POLDER II is scheduled to fly on ADEOS II in a 10:30 a.m. sun-synchronous orbit in early 2000. GERB (Geostationary Earth Radiation Budget) is a geostationary broadband instrument scheduled for launch in October 2000. Like CERES, these missions will provide Earth radiation budget observations together with estimates of coincident cloud properties. Comparisons between CERES fluxes with those from these instruments will provide an independent means of assessing uncertainties in Earth Radiation budget estimation (including calibration and radiance-to-flux conversion uncertainties). Comparisons will involve both near-instantaneous and mean flux/albedo estimates on regional and global spatial scales. Since these instruments will provide cloud information in addition to TOA fluxes, it will also be possible to perform detailed (statistical) comparisons of flux estimates for different cloud types (e.g. cumuliform, stratiform, cirrus etc.) and optical properties (thin vs thick, broken vs overcast, etc.). To perform these comparisons, the MISR and POLDER spectral fluxes will need to be converted to broadband values. This can be achieved by developing empirical narrow-to-broadband conversion factors stratified by scene type based on CERES broadband and imager narrowband (VIRS and MODIS) measurements.

4.5.2.1.5 Theoretical Simulations

A very useful complement to the data analysis methods mentioned above is the use of 1-dimensional, 2-dimensional, and 3-dimensional radiative transfer models to test concepts for ADM development and to predict their accuracy theoretically. These studies have been used to set nominal initial cloud classes for the ADMs (e.g. optical depth classes and cloud fraction classes) and to examine the accuracy expected theoretically for different approaches to conversion of radiance to flux. Examples of these studies can be found in Chambers, 1999 and Loeb et al., 1999b. Fig. 5 shows some preliminary results demonstrating how theoretical studies can be used to assess

uncertainties in TOA SW fluxes due to orbital sampling limitations. Fig. 5 compares some normalized sampling patterns for the POLDER instrument on the ADEOS spacecraft, and the CERES instrument on the TRMM and EOS-AM platforms in two different sampling modes. (Note that since TRMM is in a precessing orbit the sampling depends on the initial equator-crossing time for the month. Results shown in this paper are for a noon start.) A latitude zone from 30-31 degrees North in winter at a specific sun angle is considered. This is a case for which sampling differences are quite pronounced. In the cross-track mode the CERES instrument samples only a small portion of the view angle space. Even in Rotating Azimuth Plane (RAP) mode, the sampling is biased in this case to either the forward- (EOS-AM) or backward-scattering (TRMM) part of the angle space. POLDER, in contrast, provides almost no sampling at nadir; but a nicely balanced ring of samples along 45° view zenith angle.

The flux error associated with these sampling patterns is determined by weighting predetermined flux errors for 341 simulated cloud fields with the number of times it is sampled by the satellite, as follows: $\overline{\Delta F}(\theta_0) = \sum W_{ij} \Delta F(\theta_i, \phi_j; \theta_0)$. The theoretical flux errors were determined by applying simulated ADMs stratified by cloud fraction and 1D cloud optical depth classes to 2D model radiance fields from the SHDOM model (Evans, 1998). The weights, $W_{ij}(\theta_0)$, are a function both of satellite sampling frequency of that location over that time period and of the size of the field-of-view, and are normalized so their integral over the hemisphere is unity. The resulting bias and root-mean-square (RMS) relative flux errors are given in Fig. 2. Note in particular that the bias is of opposite sign for TRMM and EOS-AM, due to the portion of the angle space sampled. Also, except for the overcast clouds, the bias errors with POLDER sampling are much smaller. This is not the whole picture for climate studies, of course. Sampling at all solar zenith angles must be considered.

Results with Sampling

Single Solar Zenith Angle

Flux Bias and RMS relative error

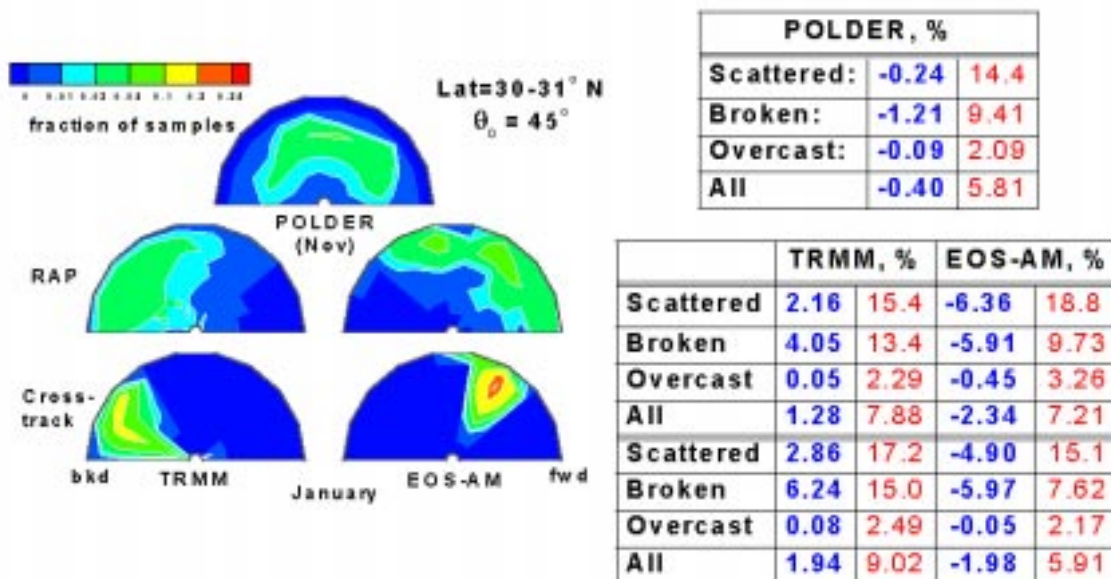


Figure 5 Sampling patterns for several satellite/instrument combinations and resulting relative flux bias and (RMS) errors for 341 cloud samples.

4.5.2.2 Sampling requirements and trade-offs

The new CERES ADMs must be constructed before they can be validated. A minimum of 18 months of CERES TRMM data is required to construct the new ADMs.

4.5.2.3 Measures of success

The purpose of increasing the number of ADM scene types is to reduce the variance within a

scene type class and thus reduce the variance of the instantaneous flux at the TOA. Our current estimate of the variance for 12 scene types is given in Table 4.5-2 as 12% standard deviation for SW. We are successful when we have defined new scene types so that the variance is reduced from 12% to 4% standard deviation. Likewise, our LW goal is reduction from 6% to 2%. Success is also measured by whether the mean and instantaneous fluxes are internally self-consistent in all viewing geometries (c.f. Section 4.5.2.1.2), and by the Direct Integration Method. For the latter, a bias in monthly average global flux of less than 0.2% SW and 0.1% LW is expected. Table 4.5-2 provides a summary of the TOA flux error budget for ERBE and that expected for CERES.

Table 4.5-2 **Error in TOA Flux due to Error in ADMs**

Parameter		Current (ERBE12 ADM)		CERES Goal (CERES 200 ADM)	
		SW	LW	SW	LW
global bias	$\sum_{\text{All data}} [E[R_i(\Omega)] - \hat{R}_i(\Omega)]$	1.0%	0.5%	0.2%	0.1%
max bias wrt Ω	$\sum_{\text{All scenes}} [E[R_i(\Omega)] - \hat{R}_i(\Omega)]$	5%	3%	1.0%	0.5%
instantaneous standard deviation for most variable scene	$\sqrt{\text{Var}[R_i(\Omega)]}$	12%	6%	4%	2%

4.5.3 PRE-LAUNCH ALGORITHM TEST/DEVELOPMENT ACTIVITIES

Pre-launch to TRMM there will be a validated set of ERBE12 ADMs. This set will be the ERBE production models (Suttles, et al., 1988, 1989). These ERBE12 ADMs will be used initially for both CERES and ERBE-like inversion. When the validated new CERES ADMs become available, all the CERES data will be reprocessed with these new ADMs.

4.5.3.1 Field experiments and studies

4.5.3.2 Operational surface networks

4.5.3.3 Existing satellite data

4.5.4 POST-LAUNCH ACTIVITIES

After 18 months of data collection, a new set of CERES ADMs will be built with CERES RAP data. These models will be validated with the Direct Integration Method using one month of CERES data. We will also test the internal self-consistency of CERES mean and instantaneous fluxes with viewing geometry (Viewing Zenith Angle Dependence Test and Along-Track Test).

4.5.4.1 Planned field activities and studies

4.5.4.2 New EOS-targeted coordinated field campaigns

4.5.4.3 Needs for other satellite data

4.5.4.4 Measurement needs at calibration/validation sites

4.5.4.5 Needs for instrument development

4.5.4.6 Geometric registration site

4.5.4.7 Intercomparisons

As described in Section 4.5.2.1.4, CERES fluxes will be compared with those from MISR, POLDER and GERB.

4.5.5 IMPLEMENTATION OF VALIDATION RESULTS IN DATA PRODUCTION

4.5.5.1 Approach

4.5.5.2 Role of EOSDIS

The operational EOSDIS SSF product will be the data source for the construction of the CERES200 ADMs. All validation tests and construction of ADMs will be done off-line.

4.5.5.3 Plans for archival of validation data

4.5.6 SUMMARY

The CERES radiances are inverted to TOA fluxes with Angular Distribution Models (ADM). CERES ADMs will be defined for scene types defined by scene parameters inferred from coincident imager retrievals. A series of consistency checks will be used to validate instantaneous and mean ADM-derived fluxes: The Direct Integration Method will be used to validate monthly mean regional radiative fluxes; the Viewing Zenith Angle Dependence Test will examine whether mean fluxes show any dependence on viewing geometry; the Along-track Test will examine the self-consistency of instantaneous fluxes with viewing geometry. Intercomparisons with other instruments providing Earth radiation budget measurements will also be performed. TOA fluxes from CERES, MISR, POLDER and GERB will be compared both on regional and global scales, and statistically by cloud type and optical property.

4.5.7 REFERENCES

- Chambers, 1999: Effect of orbital and instrument sampling pattern on error in flux retrievals. ALPS99, Meribel, France, Jan18-22, 1999, 4pp.
- Evans, K. Franklin, "The Spherical Harmonics Discrete Ordinate Method for Three-Dimensional Atmospheric Radiative Transfer," *Journal of the Atmospheric Sciences*, Vol. 55, 1 February, 1998, pp. 429-446.
- Green, R. N., J. T. Suttles, and B. A. Wielicki, 1990: Angular dependence models for radiance to flux conversion, *Proc. of SPIE*, **1299**, 102-111
- Green, R. N. and P. O'R. Hinton, 1996: Estimation of angular distribution models from radiance pairs, *J. Geophys. Res.*, **101**, 16 951-16 959.
- Loeb, N.G., and J.A. Coakley, Jr., 1998: Inference of marine stratus cloud optical depths from satellite measurements: Does 1D theory apply? *J. Climate*, **11**, 215-233.
- Loeb, N.G., and R. Davies, 1996: Observational evidence of plane parallel model biases: Apparent dependence of cloud optical depth on solar zenith angle. *J. Geophys. Res.*, **101**, 1621-1634.
- Loeb, N.G., F. Parol, J.-C. Buriez and C. Vanbauce, 1999a: Top-of-atmosphere albedo estimation from angular distribution models: Influence of biases in 1D cloud optical depth retrievals. *J. Climate*, (submitted).
- Loeb, N. et al., 1999b: Comparison between two techniques for constructing angular distribution models: theory and CERES measurements. ALPS99, Meribel, France, Jan18-22, 1999, 5pp.
- Smith, G. L., J. T. Suttles, and N. Manalo, 1989: The ERBE alongtrack scan experiment, IRS '88: Current Problems in Atmospheric Radiation, Lenoble and Geleyn, editors, 242-244, A. Deepak Publishing, Hampton.
- Smith, G. L., N. Manalo, J. T. Suttles, and I. J. Walker, 1989: Limb-darkening functions as derived from along-track operation of the ERBE scanning radiometers for January 1985, *NASA Ref. Publ. 1214*.
- Smith, G. L., N. D. Manalo, and L. M. Avis, 1990: Limb-darkening functions as derived from along-track operation of the ERBE scanning radiometers for August 1985, *NASA Ref. Publ. 1243*.
- Suttles, J. T., R. N. Green, P. Minnis, G. L. Smith, W. F. Staylor, B. A. Wielicki, I. J. Walker, D. F. Young, V. R. Taylor, and L. L. Stowe, 1988: Angular radiation models for Earth-atmosphere system. Part I: Shortwave radiation, NASA Reference Publication 1184, Vol. I.
- Suttles, J. T., R. N. Green, G. L. Smith, B. A. Wielicki, I. J. Walker, V. R. Taylor, and L. L. Stowe, 1989: Angular radiation models for the Earth-atmosphere system. Part II: Longwave radiation, NASA Reference Publication 1184, Vol. II.
- Suttles, J. T., B. A. Wielicki, and S. Vemury, 1992: Top-of-atmosphere radiative fluxes: Validation of ERBE scanner inversion algorithm using *Nimbus-7* ERB data, *J. Appl. Meteor.*, **31**, 784-796.
- Wielicki, B. A., and R. N. Green, 1989: Cloud identification for ERBE radiation flux retrieval, *J. Appl. Meteor.*, **28**, 1133-1146.
- Wielicki, B. A., R. D. Cess, M. D. King, D. A. Randall, and E. F. Harrison, 1995: Mission to planet earth: Role of clouds and radiation in climate, *Bull. Am. Meteor. Soc.*, **65**, 2125-2153.

CERES VALIDATION
CERES INVERSION
TO INSTANTANEOUS TOA FLUXES

DATA PRODUCTS/PARAMETERS

CERES Product: SSF. Parameters: TOA flux, CERES ADMs.

MISSIONS

TRMM, EOS AM-1, EOS PM-1

APPROACH

Test ADMs with Direct Integration Method (monthly regional means)

Along-track Test (instantaneous flux consistency)

Viewing Zenith Angle Dependence Test (monthly mean consistency)

CERES-MISR-POLDER-GERB (compare to independent data)

PRE-LAUNCH

Validate ERBE12 ADMs for initial CERES inversion.

POST-LAUNCH

Validate CERES ADMs.

Intercompare CERES-MISR-POLDER-GERB fluxes.

EOSDIS

EOSDIS SSF product is data source. All validation tests off-line.